Atmospheric Environment 94 (2014) 671–679

Contents lists available at ScienceDirect

Atmospheric Environment

journal homepage: www.elsevier.com/locate/atmosenv

Widespread reductions in haze across the United States from the early 1990s through 2011

J.L. Hand [a, *], B.A. Schichtel [b], W.C. Malm [a], S. Copeland [a], J.V. Molenar [c], N. Frank [d], M. Pitchford [e]

[a] Cooperative Institute for Research in the Atmosphere, Colorado State University, Fort Collins, CO 80523, USA
[b] National Park Service, Cooperative Institute for Research in the Atmosphere, Colorado State University, Fort Collins, CO 80523, USA
[c] Air Resource Specialists, 1901 Sharp Point Drive, Suite E, Fort Collins, CO 80525, USA
[d] Air Quality Assessment Division, U.S. Environmental Protection Agency, Research Triangle Park, NC 27711, USA
[e] Division of Atmospheric Sciences, Desert Research Institute, Reno, NV 89512, USA

HIGHLIGHTS

- Trends in the reconstructed mean 20% haziest extinction were computed.
- Trends were computed at remote sites across the United States since 1990s.
- Simulated images of national parks show dramatic improvement in visibility.

ARTICLE INFO

Article history:
Received 20 December 2013
Received in revised form
20 May 2014
Accepted 21 May 2014
Available online 27 May 2014

Keywords:
Haze
Visibility
Aerosol trends
Remote aerosols

ABSTRACT

Visibility has improved significantly at many remote areas across the United States since the early 1990s. Trends in visibility were calculated using ambient light extinction coefficients (b_{ext}) estimated from speciated particulate concentrations measured by the IMPROVE (Interagency Monitoring of Protected Visual Environments) network. The 20% haziest b_{ext} levels were computed for each year following Regional Haze Rule guidelines and aggregated over three major regions of the United States. Over the last two decades (1992–2011) the regional mean 20% haziest b_{ext} dropped by 52% (-2.6% yr^{-1}, $p < 0.01$) in the eastern United States, and by 20% (-1.0% yr^{-1}, $p = 0.08$) for sites along the West Coast. However, in the Intermountain/Southwest region, the trend was insignificant (-0.2% yr^{-1}, $p = 0.36$). Over the last decade (2002–2011) the haziest b_{ext} in the Intermountain/Southwest region decreased by 15% (-1.5% yr^{-1}, $p = 0.09$), compared to a decrease of 35% (-3.5% yr^{-1}, $p = 0.06$) in the West Coast region and 50% (-5.0% yr^{-1}, $p = 0.02$) in the East. A novel aspect to this study is the visualization of trends through the simulation of images of national parks and other remote areas for early and current haziest conditions. These images are an effective means for communicating trends and illustrate the dramatic improvement in visibility, especially in the East, where reductions in sulfate concentrations and sulfur dioxide emissions have had a positive impact on visibility degradation. However, while conditions are clearer for regions in the West, less improvement points to the need for understanding the influences on the trends in haziest conditions in those regions.

1. Introduction

Visibility has long been considered an important aspect of air quality protection in national parks and the United States. For example, the stated purpose of the National Park Service Organic Act of 1916 was "… to conserve the scenery and the natural and historic objects and the wildlife therein and to provide for the enjoyment of the same in such a manner and by such means as will leave them unimpaired for the enjoyment of future generations" (U.S. Code 16.1.1). With the passing of the Clean Air Act (CAA) (U.S. Code 42.85) in 1970 and the formation of the Environmental Protection Agency (EPA), major regulatory programs were developed that included national ambient air quality standards (NAAQS). The CAA amendments of 1977 introduced additional protection for

* Corresponding author.
E-mail address: jlhand@colostate.edu (J.L. Hand).

http://dx.doi.org/10.1016/j.atmosenv.2014.05.062
1352-2310/

certain national treasures. One stated purpose of Part C of the amendments, Prevention of Significant Deterioration of Air Quality, was "to preserve, protect, and enhance the air quality in national parks, national wilderness areas, national monuments, national seashores, and other areas of special national or regional natural, recreational, scenic, or historical value" (U.S. Code 42.7470). These special areas were designated as class I areas (CIA) and included international parks, national wilderness areas, and national memorial parks that exceeded 5000 acres in size and national parks that exceeded 6000 acres in size in existence on the date of enactment of the 1977 CAA amendments (U.S. Code 42.7472). Section 169A of the 1977 CAA amendments declared as a national goal "… the prevention of any future, and the remedying of any existing, impairment of visibility in mandatory class I federal areas which impairment results from manmade air pollution" (U.S. Code 42.7491). Section 169B of the 1990 CAA amendments focused attention on regional haze and was specifically designed to address visibility issues by expanding visibility monitoring networks and requiring studies to investigate the formation and transport of haze (U.S. Code 42.7492). Other provisions of the 1990 amendments that were designed to reduce the impacts of air pollution on health also affect visibility. Title I addressed the designation of NAAQS non-attainment areas as well as interstate and intercontinental transport, and Title II addressed motor vehicle emissions and fuel standards. Title IV (Acid Deposition Control) established regulatory mandates to reduce electric utility emissions of sulfur dioxide (SO_2) and nitrogen dioxides (NO_x), both of which form particulates in the atmosphere that contribute to visibility degradation and to acid deposition (U.S. Code 42.7651).

The recognition of and response to interstate pollution issues led to the promulgation of the Regional Haze Rule (RHR) by the EPA in 1999 (U.S. EPA, 1999). The RHR was established to achieve the national visibility goal established by Section 169A and called for the elimination of anthropogenic visibility impairment in 156 CIAs by a target date of 2064. Specifically, the RHR calls for no increased impairment of the 20% cleanest conditions and for reasonable progress toward RHR-defined natural visibility conditions for the 20% haziest conditions. Light extinction coefficients (b_{ext}) incorporated by the RHR are reconstructed using an algorithm that accounts for the atmospheric attenuation of visible solar radiation due to scattering and absorption by major aerosol species and by molecular scattering (Rayleigh) using measurements of speciated aerosol concentrations from the Interagency Monitoring of Protected Visual Environments (IMPROVE) network (Malm et al., 1994a; Pitchford et al., 2007). The haze index in deciview units (dv), a logarithmic transformation of reconstructed b_{ext} (Pitchford and Malm, 1994), was selected to track haze levels for the RHR. Five-year periodic assessments are required from each state to evaluate its progress toward achieving natural visibility conditions by 2064 as defined by the RHR. A review of progress toward these goals for the baseline period (2000–2004) and for period 1 (2005–2009) was reported in chapter 9 of Hand et al. (2011).

Developing successful mitigation strategies to achieve regulatory goals such as the RHR requires an understanding of the major aerosol species that contribute to visibility degradation. These contributions vary both seasonally and spatially, as described in Hand et al. (2011) for 2005–2008 monthly mean reconstructed b_{ext} at the surface. In the eastern United States, extinction due to ammonium sulfate contributed 60–70% to visibility degradation on an annual basis and even higher during summer (Brewer and Adlhoch, 2005; Brewer and Moore, 2009), due to high industrial SO_2 emissions and sulfate concentrations in the region (Hand et al., 2012a). Contributions from ammonium sulfate to b_{ext} were much lower in the West (10–30%). Monthly mean contributions to reconstructed b_{ext} at the surface from particulate organic matter (POM) in the East ranged from 5% to 20%. Contributions to haze from POM were greatest in the western United States (40–70%), with the highest contributions in northern California, Montana, and Idaho, due to biomass burning and biogenic emissions (e.g., Jaffe et al., 2008; Schichtel et al., 2008; Holden et al., 2011). Major contributions from ammonium nitrate occurred in the central United States and southern California (30–40% annually and up to 50% in winter), with lower contributions in the East and Southwest (~10%). Contributions from elemental carbon (EC) were around 10% in the West and ~5% in the East. Fine soil contributions to b_{ext} were only a few percent in the East and ranged up to 10% or higher in the Southwest. Sea salt contributions were insignificant except at some coastal sites.

Changes in visual air quality over time can be quantified through trend analyses that provide an evaluation of progress toward meeting regulatory goals and gauge success of emission reduction programs. A study by Schichtel et al. (2001) reported human visual range measurements at nearly 300 meteorological stations across the United States that indicated a significant decrease in haziness from 1980 to 1995. Decadal trends in aerosol optical properties from measurements through 2010 at remote stations in the Northern Hemisphere and Antarctica suggested that light scattering by particles at most North American stations had significantly decreased since the early/mid-1990s and 2000s (Collaud Coen et al., 2013). Other studies have investigated trends in haze-causing particulates in remote regions, but not necessarily their effects on visibility or on the visual scene (Malm et al., 2002; Murphy et al., 2011; Hand et al., 2012a, 2013).

Demonstrating the impact of the change in visual air quality over time on a given scene is a powerful method for communicating trends in visibility. To this end, we simulated images of national parks and other remote areas corresponding to early and current haze levels using visualization software (Air Resource Specialists, Fort Collins, CO). Haze levels were computed following RHR guidelines for the 20% haziest reconstructed b_{ext} levels for long-term (1990–2011) and short-term (2000–2011) individual IMPROVE sites, as well as for narrowed time periods for regionally aggregated sites. Changes in IMPROVE annual mean fine particulate mass concentrations and the EPA's National Emission Inventory's total annual gaseous emissions were also evaluated. Combining the analyses of trends in haze and particulate mass concentrations and gaseous emissions with the demonstrable impacts of the changes on a scene is an effective means by which to evaluate trends in visual air quality. This evaluation is useful for assessing the national goals and regulatory programs designed to reduce particulate concentrations and thereby improve visibility at remote areas in the United States.

2. Experimental

The IMPROVE network collects 24-h samples every third day from midnight to midnight local time, and concentrations are reported at ambient conditions. Inorganic anions are analyzed by ion chromatography and are artifact corrected, carbonaceous aerosols (organic, OC, and elemental, EC) are analyzed by thermal optical reflectance (TOR) and are artifact corrected, elemental concentrations are determined by X-ray fluorescence, and $PM_{2.5}$ and PM_{10} mass concentrations are determined through gravimetric weighing. Additional details regarding IMPROVE site location, sampling, analysis methodology, and detailed descriptions of network operations and data analysis have been previously reported (Malm et al., 1994a; Hand et al., 2011, 2012b). IMPROVE data advisories were followed for the data reduction and analysis in this study (http://vista.cira.colostate.edu/improve/Data/QA_QC/Advisory.htm).

IMPROVE data are available for download (http://vista.cira.colostate.edu/IMPROVE).

The revised IMPROVE algorithm (Pitchford et al., 2007) was used to reconstruct ambient b_{ext} (Mm^{-1}) at a wavelength of 550 nm assuming an external mixture. The algorithm accounts for ambient scattering by fine ($PM_{2.5}$) particulate ammonium sulfate ($4.125 \times S$), ammonium nitrate ($1.29 \times NO_3^-$), POM ($1.8 \times OC$), sea salt ($1.8 \times Cl^-$), soil, and coarse mass ($PM_{10} - PM_{2.5}$) and for absorption by EC. It also accounts for site-specific Rayleigh scattering (~10 Mm^{-1}). Hygroscopic effects were accounted for using monthly and site-specific growth curves (f(RH)) that were generated based on monthly climatological mean RH values (U.S. EPA, 2001, 2003). The climatological RH values eliminate the effects of interannual variations in RH while maintaining typical regional and seasonal humidity patterns across the United States. Applying climatological f(RH) values avoids the influence of relative humidity on trends. Growth curves were applied only to hygroscopic species (ammonium sulfate, ammonium nitrate, and sea salt). The 20% haziest and cleanest b_{ext} were computed as the mean of the 20% highest and lowest b_{ext}, respectively, at each site for each year of complete data based on RHR completeness criteria (U.S. EPA, 2003). Previous studies have demonstrated the ability of the revised algorithm to accurately reconstruct measured b_{ext} (e.g., Malm and Hand, 2007; Pitchford et al., 2007). Reconstructed b_{ext} reported here are available for download (http://views.cira.colostate.edu/fed).

Linear Theil regression was used to compute trends in b_{ext} because it minimizes the impact of outliers on regression results (Theil, 1950). Individual site trends (% yr^{-1}) were computed by dividing the slope from the regression of b_{ext} by the median of b_{ext} over the time period of the trend and multiplying by 100%. Site-specific, long-term (1990–2011) and short-term (2000–2011) trends were computed for sites with 70% complete years over the time period considered. Short-term trends began in 2000 to take advantage of the network expansion that met RHR monitoring requirements. Trends were considered significant at the 90% level ($p < 0.10$); significance levels were computed using Kendall tau statistics. Regional trends were computed by aggregating data into three separate continental U.S. regions that included sites in the East (east of −100° longitude), the Intermountain/Southwest (−116° to −100° longitude), and the West Coast (west of −116° longitude). Sites are shown on inset maps on later figures. The regions were defined based on spatial patterns in haziest b_{ext}. Regional trends were computed by normalizing yearly b_{ext} at a given site by the median of b_{ext} over the time period of interest, then calculating the geometric mean of these normalized b_{ext} across sites within a region for each year, and finally calculating the trend on the yearly regional mean normalized b_{ext} values. Time periods for regional trends were shortened (1992–2011 and 2002–2011 for long-term (LT) and short-term (ST) sites, respectively) relative to site-specific trends to account for disparate geographical coverage, as the early years of network initiation and expansion can bias trends (Schichtel et al., 2011; Hand et al., 2012a).

The effects of the changes in the haziest b_{ext} on various scenes were simulated using the WinHaze 2.9.9.1 model (Air Resource Specialists, Fort Collins, CO). WinHaze incorporates aerosol and radiative transfer modules with image processing to synthesize images representing air quality and environmental conditions (Malm et al., 1983; Molenar et al., 1994). Model inputs require specifying either speciated particulate concentrations, species-dependent hygroscopic and optical properties (i.e., mass extinction efficiencies) and relative humidity, or measured or reconstructed aerosol optical properties such as b_{ext}. We input the haziest reconstructed b_{ext} values corresponding to the beginning and end of trend periods to illustrate changes in the scene corresponding to the calculated trends. Scenes were simulated for approximately 50 national parks and wilderness areas with valid trends in b_{ext}.

3. Haze trends

Isopleth maps of the mean 20% haziest b_{ext} for 2000 through 2002 and 2009 through 2011 are shown in Figs. 1 and 2, respectively. The same scale applies to both maps. Similar results for the 20% cleanest b_{ext} are provided in the Supplementary Material; the remaining discussion focuses on the haziest b_{ext}. Isopleths shown in the figures were generated using a Kriging algorithm and are intended to guide the eye for spatial patterns. At the beginning of the decade, the haziest visibility conditions were greater than 200 Mm^{-1} over the entire central-eastern United States, with the most extreme visibility degradation along the Ohio River valley, coinciding with the highest particulate loading (Hand et al., 2011, 2012b). The haziest conditions in the West during this period were only a fraction of those in the East, with Rayleigh scattering contributing a significant portion. The haziest conditions dropped dramatically throughout the country during the later period (Fig. 2), with the largest decreases at sites in the East and West Coast.

Trend analyses quantify the level and significance of the change. Site-by-site trends (% yr^{-1}) in the mean 20% haziest b_{ext} are shown

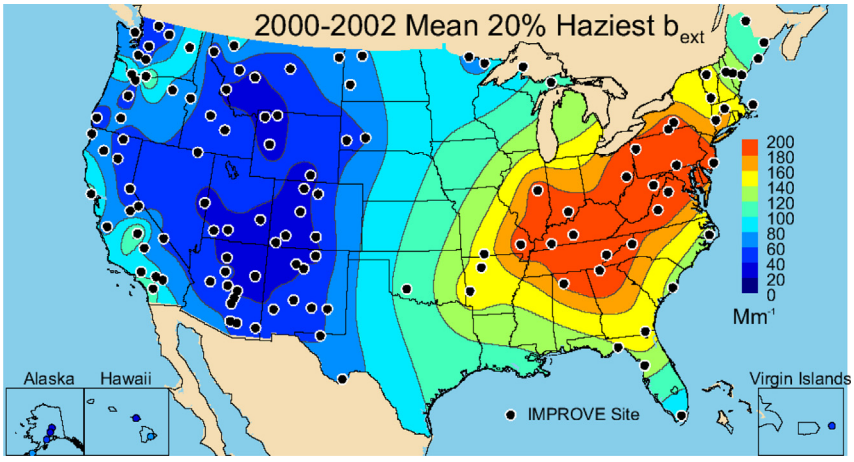

Fig. 1. IMPROVE 2000–2002 reconstructed mean 20% haziest ambient light extinction coefficient (b_{ext}, Mm^{-1}, at 550 nm), including contributions from Rayleigh scattering. IMPROVE sites are shown as black circles.

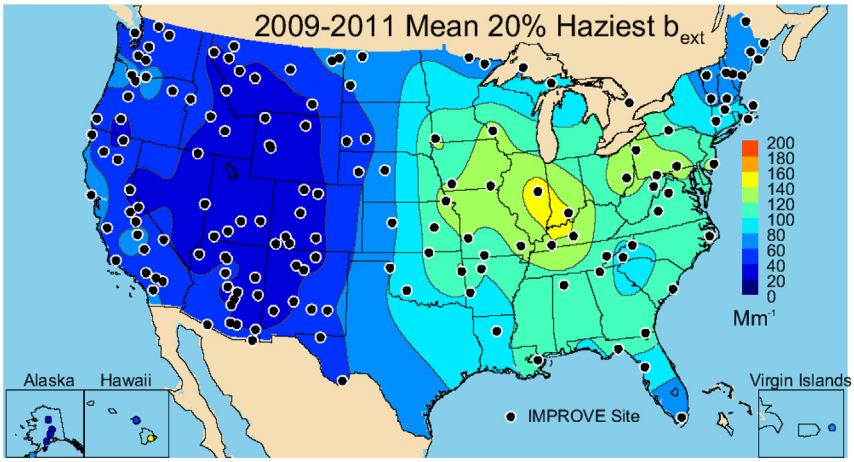

Fig. 2. IMPROVE 2009–2011 reconstructed mean 20% haziest ambient light extinction coefficient (b_{ext}, Mm^{-1}, at 550 nm), including contributions from Rayleigh scattering. IMPROVE sites are shown as black circles.

in Figs. 3 and 4 for LT sites (1990–2011) and ST sites (2000–2011), respectively. The location of triangles refers to IMPROVE site locations, with upward-pointing triangles corresponding to increased b_{ext}, and vice versa. Filled triangles correspond to statistically significant trends ($p < 0.10$); unfilled triangles correspond to insignificant trends. The number of sites nearly quadrupled from 36 to 140 for the two time periods, with more sites added to regions in the central United States and Great Plains after the network expansion.

Reductions in haziest b_{ext} at LT sites were greatest in the East where b_{ext} declined at a rate of approximately −2% to −3% yr^{-1} since 1990 (Fig. 3). The haziest conditions at western LT sites have improved at a slower rate relative to sites in the East, and several trends were positive but insignificant in the Southwest and California. The largest decrease in the haziest conditions for all LT sites (statistically significant) occurred at San Gorgonio Wilderness Area, California (−3.8% yr^{-1}, $p < 0.01$). The least amount of change occurred at Tonto National Monument, Arizona (−0.8% yr^{-1}, $p = 0.05$). Regional differences also existed for ST trends (Fig. 4), where the haziest conditions at sites in the East decreased at a rate of approximately −4% yr^{-1}or greater, but only 0 to −2% yr^{-1} in the West. A few ST sites in Oregon, the Southwest, and the northern Great Plains experienced positive, although insignificant, trends. The greatest improvement in the ST haziest conditions occurred at Cohutta, Georgia (−8.6% yr^{-1}, $p = 0.05$), while the haziest b_{ext} significantly increased at Hawaii Volcanoes, Hawaii, at a rate of 9.4% yr^{-1} ($p = 0.07$).

Regional mean trends capture the spatial differences seen in isopleths of site-specific trends and summarize the temporal behavior of haze within a region. Timelines of regional mean haziest b_{ext} for the East, Intermountain/Southwest, and West Coast are shown for narrowed time periods for LT (1992–2011) and ST (2002–2011) sites in Fig. 5 (top, middle, and lower panels, respectively). The LT and ST sites included in the regional means are shown on the inset maps in each panel. The plotting symbol corresponds to the number of complete sites for a given year with data included in the mean. Differences between ST (black) and LT (red) timelines for overlapping years reflect the geographical differences in the sites available during the given time period.

The haziest conditions in the East experienced a 52% decrease from ~200 Mm^{-1} in the early 1990s to ~100 Mm^{-1} by 2011 (−2.6% yr^{-1}, $p < 0.01$). Since 2000 the regional mean ST haziest conditions in the East decreased by 50% (−5.0% yr^{-1}, $p = 0.02$), respectively. Trends at all ST and LT sites were negative and most were significant

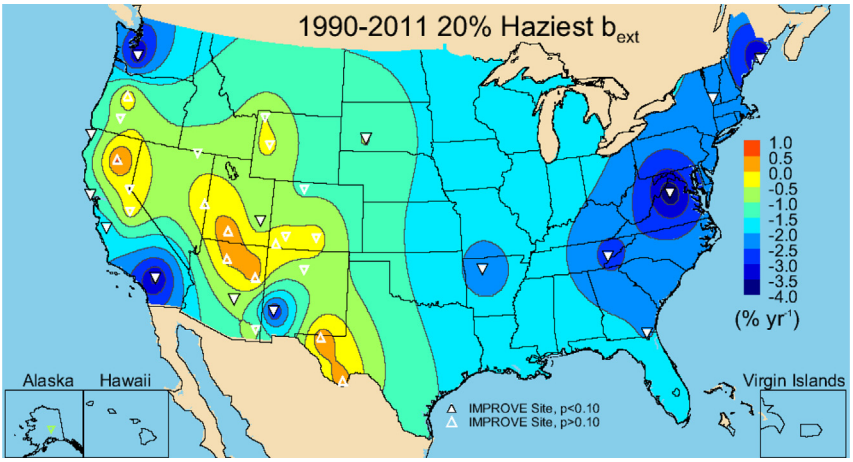

Fig. 3. IMPROVE 1990–2011 trends (% yr^{-1}) in the reconstructed mean 20% haziest ambient light extinction coefficient (b_{ext} at 550 nm). Triangles correspond to IMPROVE sites; upward-pointing triangles correspond to increased b_{ext} and vice versa. Significance levels (p) less than 0.10 are considered significant (filled triangles).

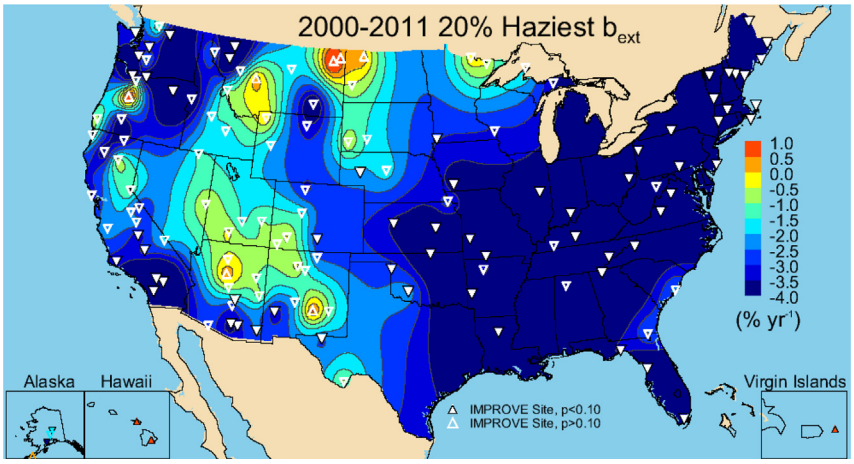

Fig. 4. IMPROVE 2000–2011 trends (% yr^{-1}) in the reconstructed mean 20% haziest ambient light extinction coefficient (b_{ext} at 550 nm). Triangles correspond to IMPROVE sites; upward-pointing triangles correspond to increased b_{ext} and vice versa. Significance levels (p) less than 0.10 are considered significant (filled triangles).

(see Table 1 for a regional trend summary). The temporal behavior of ST and LT sites was similar, with levels that dropped considerably in 2008 and remained low.

The mean haziest b_{ext} levels in the Intermountain/Southwest were only a fraction of the eastern mean values, with very little change between the beginning and current values (35–40 Mm^{-1}) and an insignificant trend (−0.2% yr^{-1}, $p = 0.36$). Since 2000 the haziest b_{ext} at ST sites decreased by 15%, with values around 40–45 Mm^{-1} over the 10-year time period (−1.5% yr^{-1}, $p = 0.09$). The ST and LT temporal patterns were generally similar except from 2005 to 2007, when b_{ext} increased at ST sites but remained flat at LT sites. All of the ST and LT sites corresponded to negative trends in this region, but nearly a quarter of trends at ST sites were insignificant (see Table 1).

The haziest conditions along the West Coast were higher than in the Intermountain/Southwest region but still only a fraction of the eastern mean b_{ext} values. Values around 60 Mm^{-1} in the early 1990s dropped by 10% to near 50 Mm^{-1} by 2011 (−1.0% yr^{-1}, $p = 0.08$). The 35% decrease in haziest regional mean b_{ext} that occurred since 2000 at ST West Coast sites (−3.5% yr^{-1}, $p = 0.06$) was more than double the decrease in the Intermountain/

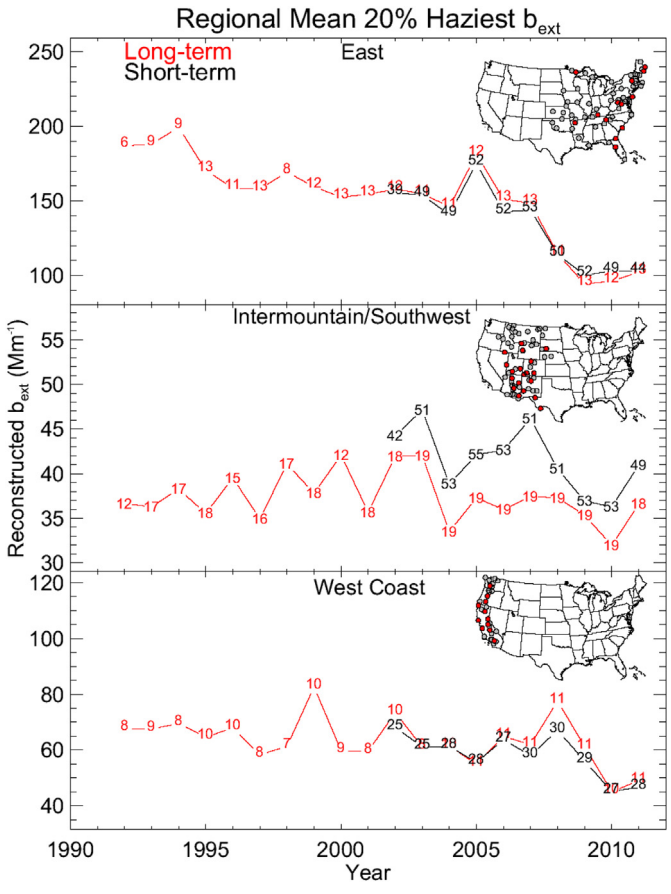

Fig. 5. Top panel: Eastern mean reconstructed 20% haziest ambient light extinction coefficient (b_{ext}, Mm^{-1}, 550 nm), including contributions from Rayleigh scattering from long-term (LT) and short-term (ST) IMPROVE sites. The number of complete sites with valid data available for a given year is used as the plot symbol for each time series. Middle panel: Intermountain/Southwest regional mean 20% haziest b_{ext}. Bottom panel: West Coast regional mean 20% haziest b_{ext}. The inset map shows regionally aggregated ST sites in gray and LT sites in red. (For interpretation of the references to colour in this figure legend, the reader is referred to the web version of this article.)

Table 1
Regional mean trends (% yr^{-1}) in the reconstructed mean 20% haziest b_{ext} for long-term (1992–2011) and short-term (2002–2011) IMPROVE sites. Trends were considered significant at $p < 0.10$.

Region[a]	East	Intermountain/ Southwest	West Coast
Long-term			
Trend (% yr^{-1})	−2.6 ($p < 0.01$)	−0.2 ($p = 0.36$)	−1.0 ($p = 0.08$)
Maximum trend (% yr^{-1})/Site	−0.8 ($p < 0.01$) Boundary Waters, MN	0.6 ($p < 0.38$) Petrified Forest, AZ	0.9 ($p = 0.33$) Lassen Volcanic, CA
Minimum trend (% yr^{-1})/Site	−4.0 ($p < 0.01$) Shenandoah, VA	−3.2 ($p < 0.01$) Gila, NM	−3.5 ($p < 0.01$) Mount Rainier, WA
Total sites	13	19	11
Number of significant positive trends	0	0	0
Number of significant negative trends	13	3	6
Short-term			
Trend (% yr^{-1})	−5.0 ($p = 0.02$)	−1.5 ($p = 0.09$)	−3.5 ($p = 0.06$)
Maximum trend (% yr^{-1})/Site	−2.0 ($p = 0.21$) Voyageurs, MN	2.3 ($p = 0.62$) Fort Peck, MT	0.7 ($p = 0.79$) Three Sisters, OR
Minimum trend (% yr^{-1})/Site	−16.8 ($p = 0.02$) Frostburg, MD	−6.6 ($p = 0.06$) Flathead, MT	−8.0 ($p < 0.01$) Agua Tibia, CA
Total sites	54	55	30
Number of significant positive trends	0	0	0
Number of significant negative trends	46	14	13

[a] See text for definition of regions.

Southwest regional mean b_{ext}. The temporal behavior in b_{ext} was similar for LT and ST sites. Although the trends were all negative, a large fraction was insignificant (see Table 1).

4. Trends in particulate concentrations and gaseous emissions

In this section we examine trends in the speciated particulate mass concentrations that contributed to haze. Trends in the particulate species that contributed to the 20% worst haze days are influenced by multiple factors, including changes in the number of days from a given season that comprise the 20% worst haze days for a given year, since the speciated $PM_{2.5}$ composition and its associated trends vary by season (e.g., Murphy et al., 2011; Hand et al., 2012a,c; Hand et al., 2013). In addition, the influence of episodic emission events, such as wild fires, varies from year to year. Consequently, trends in speciated particulate mass on the 20% worst haze days are not necessarily representative of general changes in emissions and ambient concentrations. To simplify interpretation and provide a broad context in which to interpret the haze trends we report the annual mean trends in speciated particulate matter. We also examined changes in total annual gaseous emissions.

Trends in IMPROVE aerosol concentrations were computed following similar methods outlined for haze trends and for similar regions and time periods, although only LT trends are reported. Considered were sulfate (as ammonium sulfate, $AS = 1.375 \times SO_4^{2-}$), nitrate (as ammonium nitrate, $AN = 1.29 \times NO_3^-$), total carbon ($TC = OC + EC$), and fine soil (based on elemental compounds, Malm et al., 1994a). Total annual gaseous emissions were examined because they are controlled by many of the regulatory actions described in Section 1 and because they are precursors to secondary aerosols such as ammonium sulfate and ammonium nitrate that contribute significantly to visibility degradation. The EPA's National Emission Inventory (NEI) provides emission inventories for major pollutants and source categories for the entire the United States over the past several decades (U.S. EPA, 2013). While these emissions were not region-specific, they provided an overview of the changes in overall gaseous pollutants across the United States.

Annual mean concentrations of major particulate species have generally decreased in remote areas from 1992 through 2011 (see Fig. 6 top, middle, and bottom panels for the East, Intermountain/Southwest, and West Coast regions, respectively). In the East, AS mass concentrations at the surface clearly dominated, followed by TC, AN, and soil. Annual mean AS decreased at the fastest rate (-3.1% yr^{-1}, $p < 0.01$), followed by TC (-1.8% yr^{-1}, $p < 0.01$) and AN (-1.4% yr^{-1}, $p = 0.03$). As AS declines, TC will likely contribute a larger fraction to $PM_{2.5}$ mass, as has already been demonstrated at some urban and rural sites in the Southeast (e.g. Lewandowski et al., 2007; Jimenez et al., 2009; Budisulistiorini et al., 2013). The annual mean trend in soil was fairly flat and insignificant (-0.7% yr^{-1}, $p = 0.19$).

Annual mean mass concentrations, especially of AS and TC, were lower in both western regions relative to the East. AS and TC concentrations were similar in magnitude in the Intermountain/Southwest; however, TC concentrations were highest in the West Coast region. Relative to the East, the regional, annual mean AS in the Intermountain/Southwest region decreased at a slower rate (-2.2% yr^{-1}, $p < 0.01$), but faster than that of TC (-1.4% yr^{-1}, $p = 0.02$). The LT trend in AN was flat and insignificant (-0.4% yr^{-1}, $p = 0.40$). Annual mean soil concentrations significantly increased at LT sites in the Intermountain/Southwest at a rate of 1.2% yr^{-1} ($p = 0.07$). Unique to the West Coast region, AN decreased somewhat faster than other species (-2.8% yr^{-1}, $p < 0.01$). TC and AS have decreased at the same rate at sites in the West Coast region

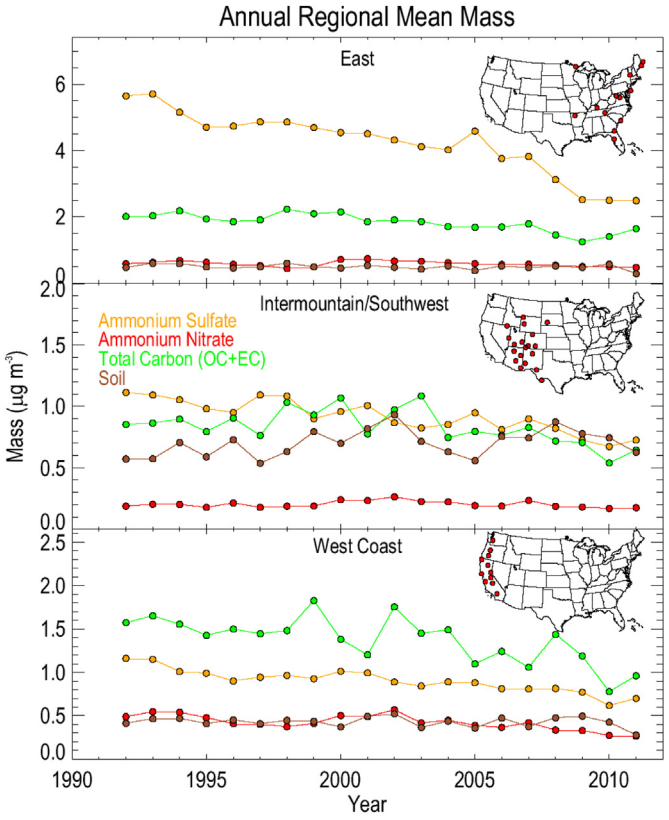

Fig. 6. Annual mean $PM_{2.5}$ mass concentrations for major aerosol species (μg m^{-3}) from long-term (LT) IMPROVE sites. Top panel: eastern regional mean, middle panel: Intermountain/Southwest regional mean, bottom panel: West Coast regional mean. The inset map shows regionally aggregated LT sites in red. (For interpretation of the references to colour in this figure legend, the reader is referred to the web version of this article.)

(-2.1% yr^{-1}, $p < 0.01$) and soil has remained fairly flat (-0.4% yr^{-1}, $p = 0.65$).

The temporal behavior of total U.S. emissions for major gaseous pollutants since 1970 (SO_2, NO_x, and volatile organic carbon, VOC) are shown in Fig. 7. Emissions have decreased steadily with the highest rates for NO_x and SO_2. Since 1990, SO_2 emissions have decreased from 23 Mtons yr^{-1} to 6 Mtons yr^{-1} in 2012, and NO_x

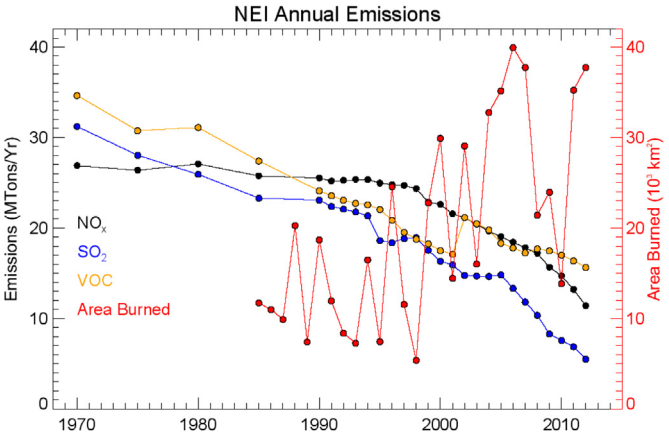

Fig. 7. National Emission Inventory (NEI) total annual United States emissions (Mtons yr^{-1}) (left axis). National Interagency Fire Center area burned (10^3 km^2) on right axis.

emissions have decreased from 26 to 11 Mtons yr^{-1} from 1990 to 2012. VOC emissions have also steadily decreased, with a step-change that reflected changes in methods used in the estimation. Also shown in Fig. 7 is the total U.S. wildfire burn area (right axis) compiled from annual total wildland fire statistics by the National Interagency Fire Center (www.nifc.gov/fireInfo/fireInfo_stats_totalFires.html). Area burned is an indication of wildfire activity and therefore smoke emissions (Spracklen et al., 2007; Jaffe et al., 2008). Clearly, while major gaseous emissions have decreased, the area burned has increased since the mid-1980s, suggesting smoke emissions also have likely increased.

5. Visibility implications and summary

Trend analyses are necessary to quantify changes in b_{ext} over time, but they do not convey the impacts of the changes on the visual appearance of a scene, similar to if one could perfectly recall a visit to a park twenty years ago and compare the view to conditions today. Images simulated with WinHaze are highly effective at communicating this change. A comparison of images created for Acadia National Park (NP), Maine, corresponding to the haziest conditions in 1990 and 2011 is shown in Fig. 8. A similar comparison is shown for Great Smoky Mountains NP, Tennessee (Fig. 9), and for San Gorgonio Wilderness, California (Fig. 10). The differences in scenes are dramatic; notice that vistas in the scenes from the early 1990s were obscured by haze but are revealed in more detail in the current scenes. Incidentally, the b_{ext} trends corresponding to the same time period in Acadia, Great Smoky Mountains, and San Gorgonio were $-3.1\%\ yr^{-1}$ ($p < 0.01$), $-3.0\%\ yr^{-1}$ ($p < 0.01$), and $-3.8\%\ yr^{-1}$ ($p < 0.01$), respectively. Images for other locations are also available (http://vista.cira.colostate.edu/IMPROVE/Studies/HazeTrends/StudyHazeTrends.htm).

The dramatic improvements in visibility at Acadia and Great Smoky Mountains were representative of the changes in conditions that occurred at many eastern sites. In the East, AS contributes a significant portion to the annual mean b_{ext} and up to 85% of the visibility degradation in summer at some sites (Hand et al., 2011). Hand et al. (2012a) demonstrated that reductions in SO_2 emissions and sulfate concentrations in the East were linearly related, and these reductions would be expected to influence visibility levels in the East (Malm et al., 1994b). It is therefore likely that the improvements in the visual scenes at eastern sites like those at Acadia and Great Smoky Mountains were largely due to the reduction of SO_2 emissions and particulate sulfate.

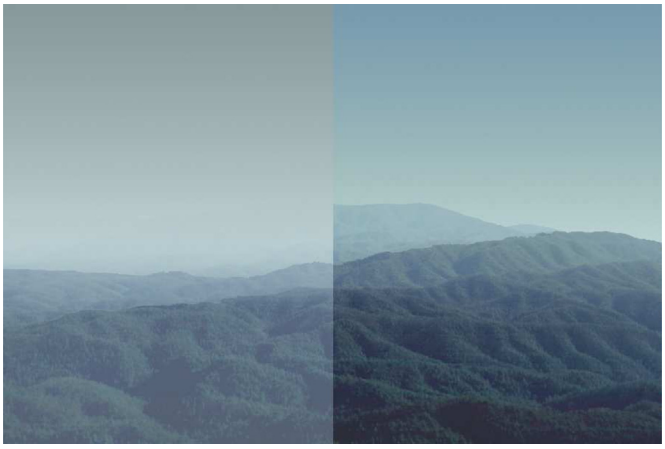

Fig. 9. Simulations of the view at Great Smoky Mountains National Park, TN, corresponding to the mean 20% haziest b_{ext} in 1990 (left, $b_{ext} = 302\ Mm^{-1}$) and 2011 (right, $b_{ext} = 114\ Mm^{-1}$). Contributions from Rayleigh scattering are included.

In the West the relationship between haze trends, changes in particulate concentrations, and gaseous emissions was more ambiguous. The reduction in haziest b_{ext} at San Gorgonio in California was impressive, but generally not representative of changes in the view at most western sites, in part because they were already fairly clean. Reductions in NO_x emissions and AN concentrations along the West Coast likely contributed to the striking improvement in visibility conditions at San Gorgonio because of the importance of AN to the extinction budget (40–50% of b_{ext} seasonally, Hand et al., 2011). Regulated SO_2 emissions have decreased in the West both annually and seasonally; however, AS concentrations have actually increased during certain seasons. Many western sites have experienced increased AS concentrations during spring, and during winter at sites in the northern and central Great Plains (Hand et al., 2012a, 2012c). The lack of linearity between SO_2 emission reductions and AS concentrations in the West suggested other influences on sulfate trends, such as international contributions or meteorological influences (Hand et al., 2012a, 2012c). The increased winter AS concentrations at sites in the Great Plains discussed in Hand et al. (2012c) coincided with positive, though insignificant, trends in ST haziest b_{ext} at the sites shown in Fig. 4.

Fig. 8. Simulations of the view at Acadia National Park, ME, corresponding to the mean 20% haziest b_{ext} in 1990 (left, $b_{ext} = 140\ Mm^{-1}$) and 2011 (right, $b_{ext} = 67\ Mm^{-1}$). Contributions from Rayleigh scattering are included.

Fig. 10. Simulations of the view at San Gorgonio Wilderness, CA, corresponding to the mean 20% haziest b_{ext} in 1990 (left, $b_{ext} = 148\ Mm^{-1}$) and 2011 (right, $b_{ext} = 50\ Mm^{-1}$). Contributions from Rayleigh scattering are included.

At many sites in the West, TC contributed a similar fraction to b_{ext} as AS on an annual basis and dominated b_{ext} during wildfire season (Hand et al., 2011). Wildfire activity has increased (Fig. 7), as have EC and TC concentrations in remote areas in the West in summer (Murphy et al., 2011; Hand et al., 2013). The smoke associated with increased acreage burned could potentially influence the haziest b_{ext}, especially during major episodes. Soil concentrations also have increased significantly in the Intermountain/Southwest, and soil can contribute up to 10–20% seasonally to b_{ext} at sites in the Southwest (Hand et al., 2011). In considering the various impacts from different species on b_{ext}, recall that visibility estimates depend not just on particulate concentrations but also on a species' optical efficiency and hygroscopic properties. Unlike AS and AN, TC and soil are weakly to non-hygroscopic, respectively.

The widespread decrease in the haziest conditions and the dramatic improvement in scenic clarity, especially in the eastern United States, points to the success of the combined regulatory activity that has resulted in reduced SO_2 and NO_x emissions and therefore secondary aerosol concentrations in the United States. However, because conditions in the West were initially cleaner and thus closer to natural background levels (~20 Mm^{-1} in the West and ~30 Mm^{-1} in the East for the haziest conditions), improvements in the haziest b_{ext} have not been as significant; in fact, at some sites the haziest conditions have actually increased. As emissions from regulated sources continue to decline, the relative contributions to visibility degradation from other sources such as wildfire emissions, dust, oil and gas extraction, and international contributions are likely to increase. The role of these sources requires more research to fully understand and predict in the context of regional haze goals.

Acknowledgments

This work was funded by the National Park Service under contract H2370094000. The assumptions, findings, conclusions, judgments, and views presented herein are those of the authors and should not be interpreted as necessarily representing the National Park Service policies. We thank Jim Renfro at Great Smoky Mountains National Park for useful discussions.

Appendix A. Supplementary data

Supplementary data related to this article can be found at http://dx.doi.org/10.1016/j.atmosenv.2014.05.062.

References

Air Resource Specialists, Website, WinHaze, http://www.air-resource.com/resources/downloads.html (accessed 12.12.13.).

Brewer, P.F., Adlhoch, J.P., 2005. Trends in speciated fine particulate matter and visibility across monitoring networks in the southeastern United States. J. Air Waste Manage. Assoc. 55, 1663–1674.

Brewer, P., Moore, T., 2009. Source contributions to visibility impairment in the southeastern and western United States. J. Air Waste Manage. Assoc. 59, 1070–1081.

Budisulistiorini, S.H., Canagaratna, M.R., Croteau, P.L., Marth, W.J., Baumann, K., Edgerton, E.S., Shaw, S.L., Knipping, E.M., Worsnop, D.R., Jayne, J.T., Gold, A., Surratt, J.D., 2013. Real-time continuous characterization of secondary organic aerosol derived from isoprene epoxydiols in downtown Atlanta, Georgia, using the Aerodyne Aerosol Chemical Speciation Monitor. Environ. Sci. Technol. 47, 5686–5694 http://dx.doi.org/10.1021/es400023n.

Collaud Coen, M., et al., 2013. Aerosol decadal trends – part 1: in-situ optical measurements at GAW and IMPROVE stations. Atmos. Chem. Phys. 13, 869–894, 105194/acp-13-869-2013.

Hand, J.L., et al., 2011. IMPROVE (Interagency Monitoring of Protected Visual Environments): Spatial and seasonal patterns and temporal variability of haze and its constituents in the United States: Report V. CIRA Report ISSN: 0737-5352-87. http://vista.cira.colostate.edu/improve/Publications/Reports/2011/2011.htm.

Hand, J.L., Schichtel, B.A., Malm, W.C., Pitchford, M.L., 2012a. Particulate sulfate ion concentration and SO_2 emission trends in the United States from the early 1990s through 2010. Atmos. Chem. Phys. 12, 10353–10365 http://dx.doi.org/10.5194/acp-12-10353-2012.

Hand, J.L., Schichtel, B.A., Pitchford, M., Malm, W.C., Frank, N.H., 2012b. Seasonal composition of remote and urban fine particulate matter in the United States. J. Geophys. Res. 117, DO5209 http://dx.doi.org/10.1029/2011JD017122.

Hand, J.L., Gebhart, K.A., Schichtel, B.A., Malm, W.C., 2012c. Increasing trends in wintertime particulate sulfate and nitrate ion concentrations in the Great Plains of the United States (2000–2010). Atmos. Environ. 55, 107–110.

Hand, J.L., Schichtel, B.S., Malm, W.C., Frank, N.H., 2013. Spatial and temporal trends in $PM_{2.5}$ organic and elemental carbon across the United States. Advanc. Meteor. 2013. Article ID 367674.

Holden, A.S., Sullivan, A.P., Munchak, L.A., Kreidenweis, S.M., Schichtel, B.A., Malm, W.C., Collett Jr., J.L., 2011. Determining contributions of biomass burning and other sources of fine particle contemporary carbon in the western United States. Atmos. Environ. 45, 1986–1993 http://dx.doi.org/10.1016/j.atmosenv.2011.01.021.

Jaffe, D., Hafner, W., Chand, D., Westerling, A., Spracklen, D., 2008. Interannual variations in $PM_{2.5}$ due to wildfires in the western United States. Environ. Sci. Technol. 42, 2812–2818.

Jimenez, J.L., et al., 2009. Evolution of organic aerosols in the atmosphere. Science 326, 1525–1529.

Lewandowski, M., Jaoui, M., Kleindienst, T.E., Offenberg, J.H., Edney, E.O., 2007. Composition of $PM_{2.5}$ during the summer of 2003 in Research Triangle Park, North Carolina. Atmos. Environ. 41, 4073–4083.

Malm, W.C., Molenar, J.V., Chan, L.Y., 1983. Photographic simulation techniques for visualizing the effect of uniform haze on a scenic resource. J. Air Pollut. Control Assoc. 33, 126–129.

Malm, W.C., Sisler, J.F., Huffman, D., Eldred, R.A., Cahill, T.A., 1994a. Spatial and seasonal trends in particulate concentration and optical extinction in the United States. J. Geophys. Res. 99 (D1), 1347–1370.

Malm, W.C., Trijonis, J., Sisler, J., Pitchford, M., 1994b. Assessing the effect of SO_2 emission changes on visibility. Atmos. Environ. 28 (5), 1023–1034.

Malm, W.C., Schichtel, B.A., Ames, R.B., Gebhart, K.A., 2002. A 10-year spatial and temporal trend of sulfate across the United States. J. Geophys. Res. 107 (D22), 4627 http://dx.doi.org/10.1029/2002JD002107.

Malm, W.C., Hand, J.L., 2007. An examination of the physical and optical properties of aerosols collected in the IMPROVE program. Atmos. Environ. 41, 3407–3427.

Molenar, J.V., Malm, W.C., Johnson, C.E., 1994. Visual air quality simulation techniques. Atmos. Environ. 28, 1055–1063.

Murphy, D.M., Chow, J.C., Leibensperger, E.M., Malm, W.C., Pitchford, M., Schichtel, B.A., Watson, J.G., White, W.H., 2011. Decreases in elemental carbon and fine particulate mass in the United States. Atmos. Chem. Phys. 11, 4679–4686 http://dx.doi.org/10.5194/acp-11-4679-2011.

Pitchford, M.L., Malm, W.C., 1994. Development and applications of a standard visual index. Atmos. Environ. 28 (5), 1049–1054.

Pitchford, M., Malm, W., Schichtel, B., Kumar, N., Lowenthal, D., Hand, J., 2007. Revised algorithm for estimating light extinction from IMPROVE particle speciation data. J. Air Waste Manage. Assoc. 57, 1326–1336, 3155/1047-3289.57.11.1326.

Schichtel, B.A., Husar, R.B., Falke, S.R., Wilson, W.E., 2001. Haze trends over the United States, 1980–1995. Atmos. Environ. 35, 5205–5210.

Schichtel, B.A., Malm, W.C., Bench, G., Fallon, S., McDade, C.E., Chow, J.C., Watson, J.G., 2008. Fossil and contemporary fine particulate carbon fractions at 12 rural and urban sites in the United States. J. Geophys. Res. 113, D02311 http://dx.doi.org/10.1029/2007JD008605.

Schichtel, B.A., Pitchford, M.L., White, W.H., 2011. Comments on "Impact of California's Air Pollution Laws on Black Carbon and their Implications for Direct Radiative Forcing" by R. Hahadur et al. Atmos. Environ. 45, 4116–4118.

Spracklen, D.V., Logan, J.A., Mickley, L.J., Park, R.J., Yevich, R., Westerling, A.L., Jaffe, D., 2007. Fires drive interannual variability of organic carbon aerosol in the western U.S. in summer. Geophys. Res. Lett. 34, L16816 http://dx.doi.org/10.1029/2007GL030037.

Theil, H., 1950. A rank-invariant method of linear and polynomial regression analysis. Proc. Kon. Ned. Adad. V. Wetensch. A 53, 386–392, 521-525, 1397-1412.

U.S. Code Title 16, Subchapter1, Sect. 1, "National Park Service Organic Act", http://www.gpo.gov/fdsys/pkg/USCODE-2011-title16/pdf/USCODE-2011-title16-chap1-subchapI-sec1.pdf, (accessed 12.12.13.).

U.S. Code Title 42, Chapter 85, "Air Pollution Prevention and Control"http://www.gpo.gov/fdsys/pkg/USCODE-2008-title42/pdf/USCODE-2008-title42-chap85.pdf, (accessed 12.12.13.).

U.S. Code Title 42, Sect. 7470, "Prevention of Significant Deterioration of Air Quality", http://www.gpo.gov/fdsys/pkg/USCODE-2010-title42/pdf/USCODE-2010-title42-chap85-subchapI-partC-subparti-sec7470.pdf, (accessed 12.12.13.).

U.S. Code Title 42, Sect. 7472, "Prevention of Significant Deterioration of Air Quality, Initial classifications", http://www.gpo.gov/fdsys/pkg/USCODE-2010-title42/pdf/USCODE-2010-title42-chap85-subchapI-partC-subparti-sec7472.pdf, (accessed 12.12.13).

U.S. Code Title 42, Sect. 7491, "Visibility protection for Federal class 1 areas", http://www.gpo.gov/fdsys/pkg/USCODE-2010-title42/pdf/USCODE-2010-title42-chap85-subchapI-partC-subpartii-sec7491.pdf, (accessed 12.12.13).

U.S. Code Title 42, Sect. 7492, "Prevention of Significant Deterioration of Air Quality, Initial classifications, Visibility protection", http://www.gpo.gov/fdsys/pkg/USCODE-2010-title42/pdf/USCODE-2010-title42-chap85-subchapI-partC-subpartii-sec7492.pdf, (accessed 12.12.13).

U.S. Code Title 42, Sect. 7651, "Air Pollution Prevention and Control-Acid Deposition Control", http://www.gpo.gov/fdsys/pkg/USCODE-2010-title42/pdf/USCODE-2010-title42-chap85-subchapIV-A-sec7651.pdf, (accessed 12.12.13).

U.S. EPA, 1999. Regional Haze Rule Regulations. Final Rule, 40 CFR 51, Federal Register, 64, pp. 35714–35774. http://www.epa.gov/ttn/caaa/t1/fr_notices/rhfedreg.pdf (accessed 12.12.13.).

U. S. EPA, 2001. Interpolating Relative Humidity Weighting Factors to Calculate Visibility Impairment and the Effects of IMPROVE Monitor Outliers, 68-D-98-113, WA No. 3-39. http://vista.cira.colostate.edu/improve/Publications/GuidanceDocs/DraftReportSept20.pdf (accessed 12.12.13.).

U.S. EPA, 2003. Guidance for Tracking Progress under the Regional Haze Rule, 68-D-02-0261. http://www.epa.gov/ttnamti1/files/ambient/visible/tracking.pdf (accessed 12.12.13.).

U.S.EPA, 2013. Technology Transfer Network Clearinghouse for Inventories and Emission Factors, National Emissions Inventory (NEI) Air Pollutant Emissions Trends Data. http://www.epa.gov/ttnchie1/trends (accessed 12.12.13.).